Shashlik calorimeters for the ENUBET tagged neutrino beam

IOP Conf. Series: Journal of Physics: Conf. Series 1162 (2019) 012032 doi:10.1088/1742-6596/1162/1/012032

Shashlik calorimeters for the ENUBET tagged neutrino beam

G Ballerini[1,2], A Berra[1,2], R Boanta[2,3], M Bonesini[2], C Brizzolari[1,2], G Brunetti[4], M Calviani[5], S Carturan[6], M G Catanesi[7], S Cecchini[8], F Cindolo[8], A Coffani[2,3], G Collazuol[4,9], E Conti[4], F Dal Corso[4], C Delogu[2,3], G De Rosa[10], A Gola[11], R A Intonti[7], C Jollet[12], Y Kudenko[13], M Laveder[4,9], A Longhin[4,9], P F Loverre[14,5], L Ludovici[15], L Magaletti[7], G Mandrioli[8], A Margotti[8], V Mascagna[1,2], N Mauri[8], A Meregaglia[16], M Mezzetto[4], M Nessi[5], A Paoloni[17], M Pari[4,9], E Parozzi[2,3], L Pasqualini[8,18], G Paternoster[11], L Patrizii[8], C Piemonte[11], M Pozzato[8], M Prest[1,2], F Pupilli[4], E Radicioni[7], C Riccio[10,19], A C Ruggieri[10], G Sirri[8], M Soldani[1,2], M Tenti[8], F Terranova[2,3], M Torti[2,3], E Vallazza[20], M Vesco[6] and L Votano[17]

[1] Phys. Dep., Università degli studi dell'Insubria, via Valeggio 11, Como, Italy
[2] INFN Sezione di Milano-Bicocca, piazza della Scienza 3, Milano, Italy
[3] Phys. Dep. Università di Milano-Bicocca, piazza della Scienza 3, Milano, Italy
[4] INFN Sezione di Padova, via Marzolo 8, Padova, Italy
[5] CERN, Geneva, Switzerland
[6] INFN Laboratori Nazionali di Legnaro, Viale dell'Università 2, Legnaro (PD), Italy
[7] INFN Sezione di Bari, via Amendola 173, Bari, Italy
[8] INFN Sezione di Bologna, viale Berti-Pichat 6/2, Bologna, Italy
[9] Phys. Dep. Università di Padova, via Marzolo 8, Padova, Italy
[10] INFN Sezione di Napoli, via Cinthia, 80126, Napoli, Italy
[11] Fondazione Bruno Kessler (FBK) and INFN TIFPA, Trento, Italy
[12] IPHC, Université de Strasbourg, CNRS/IN2P3, Strasbourg, France
[13] Institute of Nuclear Research of the Russian Academy of Science, Moscow, Russia
[14] Phys. Dep. Università La Sapienza, piazzale A. Moro 2, Rome, Italy
[15] INFN Sezione di Roma 1, piazzale A. Moro 2, Rome, Italy
[16] CENBG, Université de Bordeaux, CNRS/IN2P3, 33175 Gradignan, France
[17] INFN Laboratori Nazionali di Frascati, via Fermi 40, Frascati (Rome), Italy
[18] Phys. Dep. Università di Bologna, viale Berti-Pichat 6/2, Bologna, Italy
[19] Phys. Dep. Università degli Studi di Napoli Federico II, via Cinthia, 80126, Napoli, Italy
[20] INFN Sezione di Trieste, via Valerio, 2, Trieste, Italy

E-mail: claudia.brizzolari@gmail.com

Abstract. Shashlik calorimeters equipped with a compact readout based on Silicon PhotoMultipliers can be longitudinally segmented by directly coupling the WLS fibers with the photosensors thus embedding the readout in the bulk of the calorimeter. Results on energy resolution and particle identification for such calorimeters are presented. The SiPMs for the readout have also been characterized after being exposed to neutron fluences up to 2×10^{11} n/cm^2 (1 MeV eq.). Alternative options for the active material were also investigated; we studied in particular polysiloxane as a substitute for plastic scintillator.

1. Introduction

Shashlik calorimeters are sampling calorimeters in which the light collection is performed by WLS fibers that cross perpendicularly the tiles of absorbing and scintillating material [1], [2]. The shashlik technology is cost effective and well established, resulting in detectors with good and tunable energy resolution, by choosing the proper absorbing/scintillating tiles thickness and fiber density. However, the WLS fibers are traditionally bundled at the end of the calorimeter, thus limiting the granularity of the longitudinal sampling. For the ENUBET project [3], [4], shashlik calorimeters are combined with a compact readout based on SiPMs, thus avoiding the fiber bundling; each WLS fiber is coupled with a SiPM mounted on a custom PCB and embedded in the calorimeter structure.

In ENUBET, the calorimeters are required to perform a precise measurement of the ν_e flux originating from K_{e3} decays ($K^+ \to e^+\pi^0\nu_e$) by monitoring the positron production inside the decay tunnel of conventional neutrino beams. A longitudinal segmentation of about 4 X_0 is needed to separate the positrons from the background of charged pions. The building block of the ENUBET calorimeters is the Ultra Compact Module (UCM) (Fig. 1, 2), a shashlik calorimeter of 4.3 X_0, with iron-plastic scintillator 3×3 cm^2 tiles and read by 9 SiPMs hosted on a custom PCB. A 3D printed plastic mask precisely couples the SiPMs to one end of the fibers. The SiPMs on the PCB are connected in parallel and the current is read out without amplification.

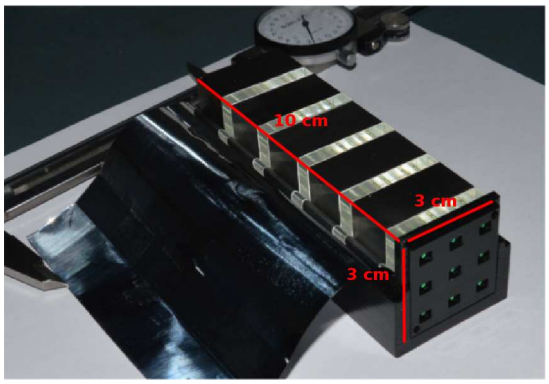

Figure 1. Ultra Compact Module; its dimensions are 3×3×10 cm^3.

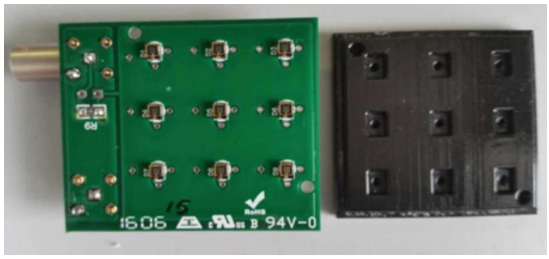

Figure 2. Printed Circuit Board and 3D printed plastic mask.

2. The ENUBET reference prototype

In November 2016 the ENUBET collaboration tested a supermodule at the CERN PS-T9 beamline, with a mixed beam of e^-, μ^-, π^- [5]. The prototype consisted of an electromagnetic calorimeter of 30.1 X_0, made of 56 UCMs arranged on 7 layers of 8 UCMs each in a 4×2 array, and an energy tail catcher read by 18 channels that covered 25.8 X_0 and had no transversal or longitudinal segmentation (Fig. 3, 4).

Zinc coated iron was chosen as the absorbing material, with 15 mm thick tiles. The 5 mm thick scintillator tiles were built from EJ-200 plastic scintillator. These tiles were coated with a TiO_2 based paint to increase the light collection efficiency; compared to more conventional techniques (e.g. insertion of Tyvek® foils between the tiles), painting is a good compromise between light collection and ease of construction [7]. The SiPMs by AdvanSiD [8] have 20×20 μm^2 cell size, breakdown at 28 V and a sensitive area of 1×1 mm^2. Most of the SiPMs were coupled to Y11 fibers. The downstream part of the supermodule was built coupling the SiPMs with BCF92

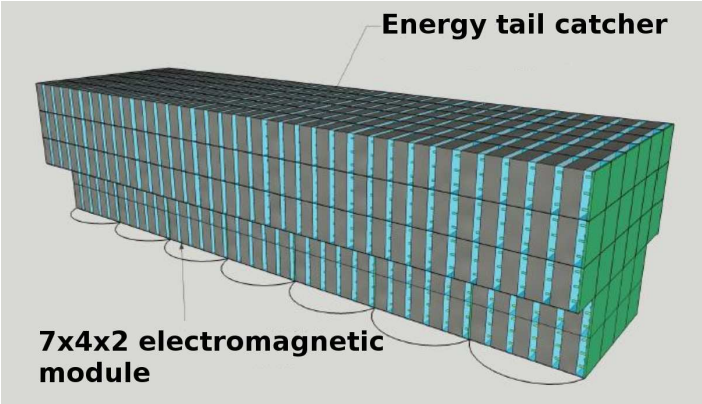

Figure 3. Layout of the reference prototype: 7 fine-grained modules and, on top, the energy tail catcher.

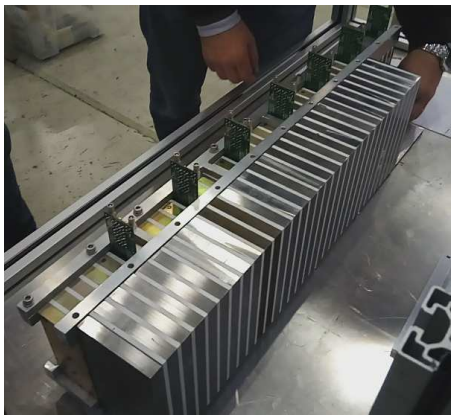

Figure 4. Photo of the calorimeter during the installation. The calorimeter is rotated by 90° with respect to the layout.

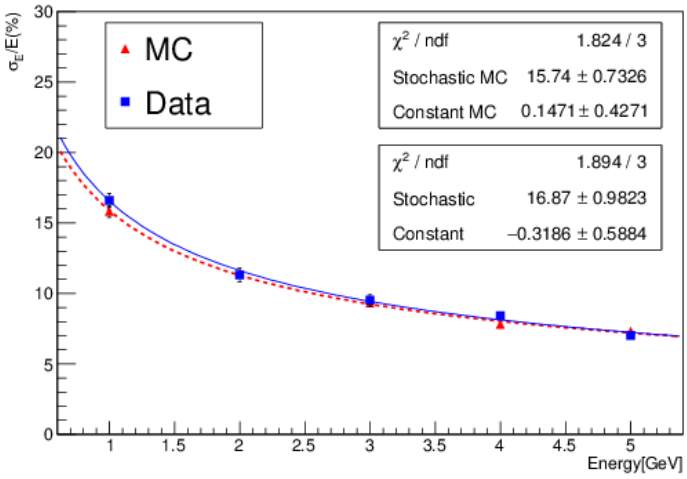

Figure 5. Energy resolution versus beam momentum for particles impinging on the calorimeter front face (0 mrad run) for data (■) and simulation (▲).

fibers.
We recorded runs with particles impinging perpendicularly on the calorimeter face (0 mrad tilt angle) and with the calorimeter tilted at 100 mrad from the beam axis, in order to simulate the angular range of interest for ENUBET. The electrons were selected with two Cherenkov counters and tracked with two pairs of $x-y$ silicon strip detectors [6] to select those impinging in a fiducial area with negligible lateral leakage.

The analysis indicates that the energy resolution is dominated by the sampling term and that the tilt of the calorimeter does not change the performance. The stochastic term in both cases is less than $20\%/\sqrt{E}$, and well within the specifications for ENUBET (Fig. 5, 6).

In ENUBET the longitudinal segmentation of the calorimeter is needed for e^+/π^+ separation

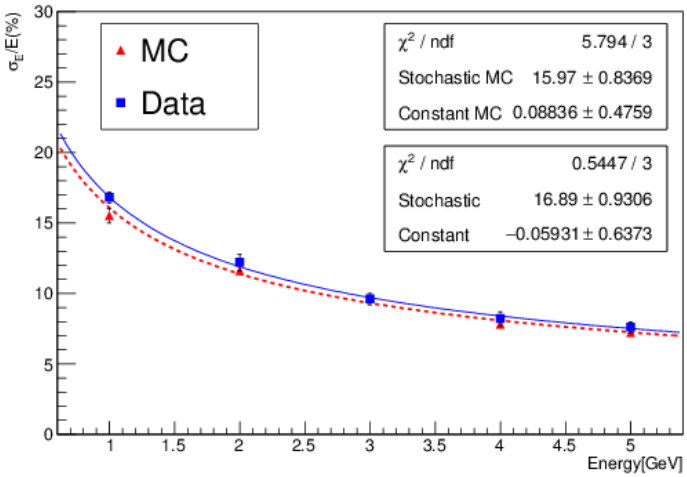

Figure 6. Energy resolution versus beam momentum for particles impinging at 100 mrad for data (■) and simulation (▲).

in the GeV energy range. The response of the calorimeter to negative pions and electrons was compared and used to validate the GEANT4 simulation. The longitudinal energy profiles of partially contained pions is reproduced by the Monte Carlo with a precision of 10% (Fig. 7).

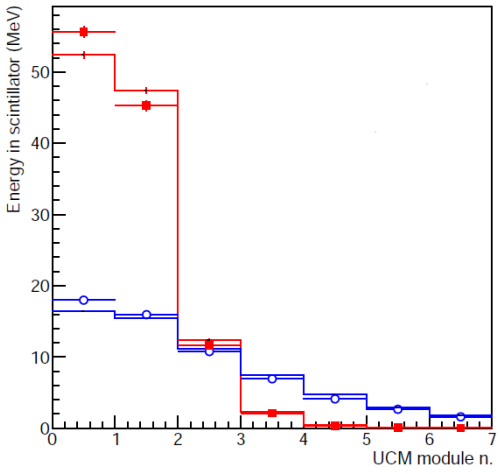

Figure 7. Average energy deposited in the scintillator as a function of the shower depth for 3 GeV pions (○: data, blue line: simulation) and electrons (■: data, red line: simulation). The depth is expressed in number of UCMs.

3. Irradiation tests

Shashlik calorimeters with embedded compact readout based on SiPMs allow to remove dead areas and inefficiencies introduced by light extraction, are very compact and can perform particle ID; however, in this design the SiPMs are exposed to fast neutrons produced by hadronic showers (Fig. 8).

We carried out irradiation tests at INFN-LNL (Laboratori Nazionali di Legnaro) in May 2017 using the CN Van de Graaff accelerator [9]. Neutrons were produced by protons (5 μA), impinging on a berillium target. We irradiated three Printed Circuit Boards (PCBs) used for

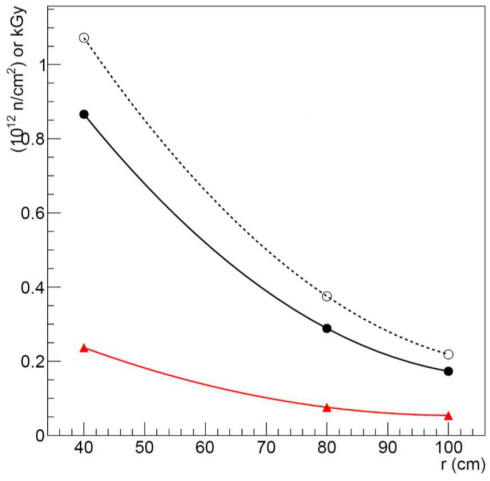

Figure 8. Ionizing (in kGy, ▲) and non-ionizing (in n/cm^2, ○, and in n-1MeV-eq/cm^2, ●) doses as a function of the distance between the axis of the ENUBET decay tunnel and the inner radius of the calorimeter.

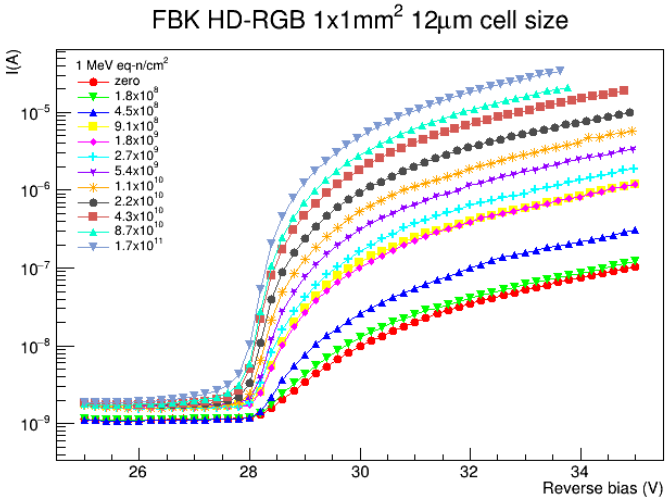

Figure 9. I-V curve of the single-SiPM PCB, 12 μm cell size.

the readout of the ENUBET UCM, hosting 9 SiPMs with a cell size of 20, 15, 12 μm. An additional PCB hosting a single 1 mm^2 SiPM with 12 μm cell size was also tested. The PCBs were equipped with a MCX connector to read the current of the SiPMs and a push-pull coaxial connector (LEMO-00) for the bias. Tests were performed up to 1.7×10^{11} n/cm^2 (1 MeV eq.) and the monitored current output for the single SiPM PCB is plotted in Fig. 9. Figure 10 displays the current of the board hosting 9 UCMs divided by 9 (i.e. normalized to a single SiPM response). The current was measured as a voltage drop through a 10 Ω resistor.

The signals collected by a non irradiated and an irradiated board were compared by exposing UCMs equipped with these boards to the mixed beam of e^-, μ^-, π^- at the CERN PS-T9 beamline. The PCBs were first installed on a UCM with 5 mm thick plastic scintillator tiles. With the irradiated board the electron peak is still visible above the pedestal peak, while the Minimum Ionizing Particle (MIP) peak is swamped by pedestal noise (Fig. 11, 12). The ratio between e^- and MIP is constant after irradiation, so the SiPMs do not display saturation due to the reduction of the working pixels. Even if MIP sensitivity is not strictly needed for ENUBET, the MIP peak can be used for real-time signal equalization and monitoring, and for

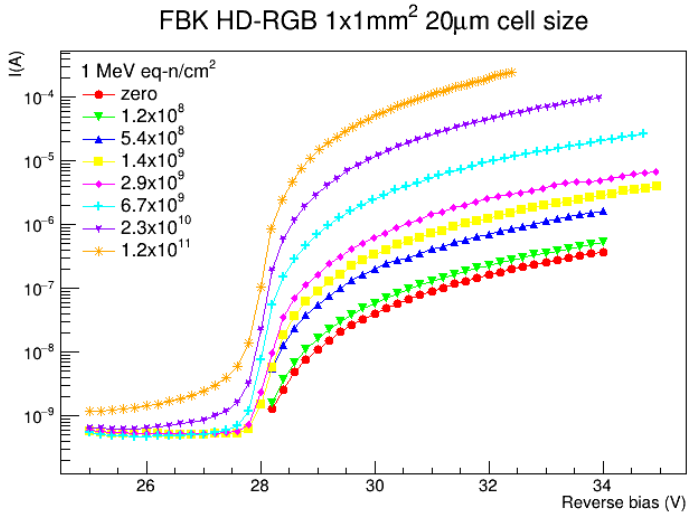

Figure 10. I-V curve of the 20 μm SiPM (current of a 9 SiPM PCB divided by 9).

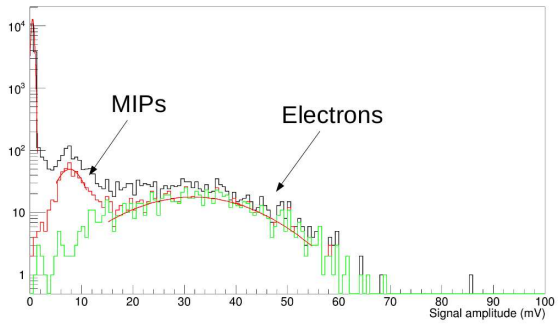

Figure 11. Signal from electrons and MIPs inside a UCM with 5 mm thick scintillator tiles, readout by a non-irradiated board.

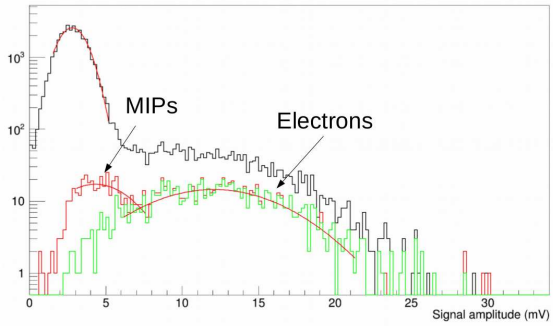

Figure 12. Signal from electrons and MIPs inside a UCM with 5 mm thick scintillator tiles, readout by an irradiated board.

the identification of muons from kaon decays and beam halo. Sensitivity to the MIP peak can be recovered increasing the scintillator thickness to 10 mm or improving the SiPM-to-fiber coupling in order to reach more than 80 p.e. per UCM. In particular, Fig. 13 shows the energy deposit inside a UCM with 13.5 mm thick scintillator tiles.

4. The polysiloxane-based calorimeter

Among alternatives to standard plastic scintillators, polysiloxane [10], [11] is particularly promising: it has a much higher hardness to ionizing doses and it is liquid at moderately high temperatures. Hence, it can be poured around the fibers between the iron slabs and cooled to room temperature. At room temperature, the scintillator is solid and optically well coupled with the fibers. Polysiloxane is particularly well suited for the construction of shashlik calorimeters because it does not require drilling or casting. On the other hand, polysiloxane based scintillators

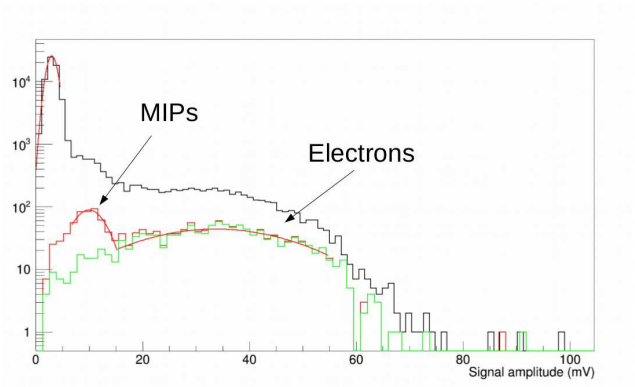

Figure 13. Signal from electrons and MIPs inside a UCM with 13.5 mm thick scintillator tiles, readout by an irradiated board.

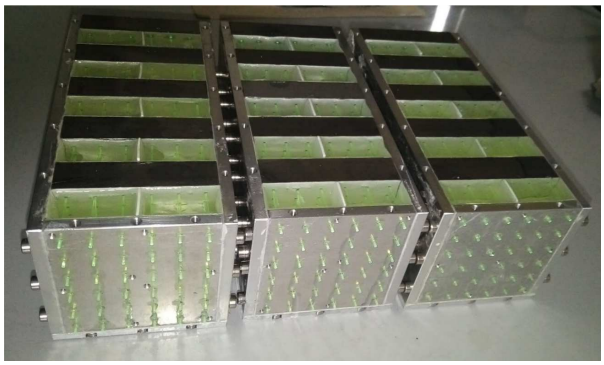

Figure 14. The three layers of the polysiloxane calorimeter, without the readout PCBs.

have a light yield that is 30% of EJ-200.

In October 2017 a ∼12 X_0 calorimeter was tested at the CERN PS-T9 beamline. The absorbing tiles were 15 mm thick as the previous prototypes, whereas the scintillating ones in polysiloxane were 15 mm thick (Fig. 14). The light collection was performed by Y11 multi-clad WLS fibers of 1 mm diameter by Kuraray. The SiPMs had a 20×20 μm^2 cell size, 1×1 mm^2 sensitive area and a breakdown at 28 V. The calorimeter consisted of 12 UCMs arranged on 3 layers of 4 UCMs each positioned in a 2×2 array in the transverse plane.

Figure 15 shows the energy resolution at different values of the overvoltage (OV, defined as the difference between the applied voltage and the breakdown voltage of 28 V). The resolution is dominated by the sampling term and the performance is similar to the calorimeter based on EJ-200.

The results showed that the quality of the scintillator-fiber coupling after cool down at room temperature is comparable with standard scintillators and the process of deposit and hardening of the scintillator does not introduce non-uniformities in the tiles (Fig. 16).

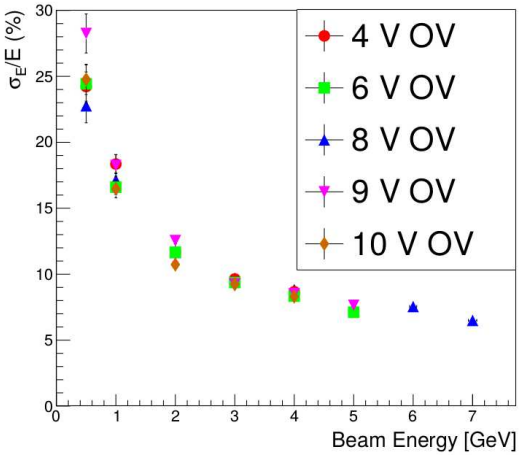

Figure 15. Energy resolution for the polysiloxane calorimeter at different overvoltages of the SiPMs.

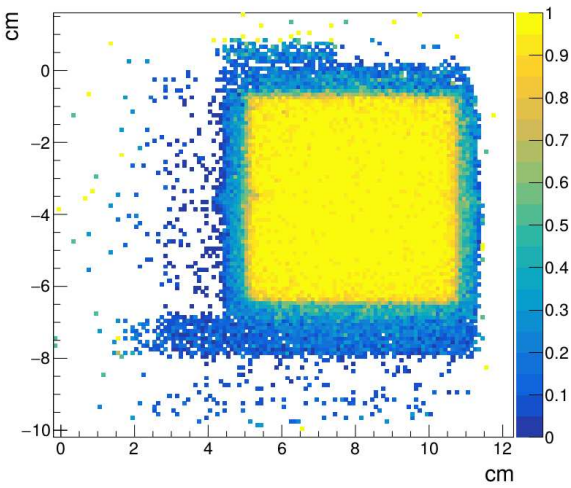

Figure 16. The efficiency map of the polysiloxane calorimeter.

References

[1] Fessler H, Freund P, Gebauer J, Glas K M, Pretzl K, Seyboth P, Seyerlein J and Thevenin J C 1985 *Nucl. Instrum. Meth.* A **228** 303
[2] Atoyan G S et al. 1992 *Nucl. Instrum. Meth.* A **320** 144
[3] Longhin A, Ludovici L and Terranova F 2015 *Eur. Phys. J.* C **75** 155
[4] Berra A et al. (ENUBET Coll.), CERN-SPSC-2016-036, SPSC-EOI-014
[5] Berra A et al. 2018 Testbeam performance of a shashlik calorimeter with fine-grained longitudinal segmentation *JINST* **13** no. 1 P01028
[6] Prest M, Barbiellini G, Bordignon G, Fedel G, Liello F, Longo F, Pontoni C and Vallazza E 2003 The AGILE silicon tracker: an innovative gamma-ray instrument for space *Nucl. Instrum. Meth.* A **501** *280*
[7] Berra A et al. 2017 Shashlik calorimeters with embedded SiPMs for longitudinal segmentation *IEEE TNS* **64** no. 4 1056
[8] Fondazione Bruno Kessler, Via Santa Croce 77, I-38100, Trento, Italy
[9] Ballerini G et al. Irradiation and performance of HD-RGB SiPM for calorimetric applications, in preparation.
[10] Carturan S et al. 2010 Novel polysiloxane-based scintillators for neutron detection *Radiation protection dosimetry* **143** 471-6
[11] Quaranta A et al. 2011 Doped polysiloxane scintillators for thermal neutrons detection *Journal of Non-Crystalline Solids* **357** no. 8-9 1921-5